Chem Biol Drug Des 2015; **86:** 764–775

Research Article

Design, Synthesis and *in vivo* Evaluation of Novel *C*-Aryl Glucosides as Potent Sodium-Dependent Glucose Cotransporters Inhibitors for the Treatment of Diabetes

Zheng Li[1], Xuekun Wang[1], Xue Xu[2], Qianqian Qiu[1], Lei Jiao[1], Wenlong Huang[1,*] and Hai Qian[1,*]

[1]Center of Drug Discovery, State Key Laboratory of Natural Medicines, China Pharmaceutical University, 24 Tongjiaxiang, Nanjing 210009, China
[2]Key Laboratory of Drug Quality Control and Pharmacovigilance, China Pharmaceutical University, 24 Tongjiaxiang, Nanjing 210009, China
**Corresponding authors: Wenlong Huang, ydhuangwenlong@126.com*; Hai Qian, *qianhai24@163.com*

A series of novel *C*-aryl glucosides with substituents at the 3′-position or cyclization at 3′, 4′-positions of the distal aryl ring were designed and synthesized, which might decrease the oxidative metabolism of dapagliflozin. Preliminary evaluation for hypoglycemic effect and the risk of hypoglycemia were carried out both in normal and in streptozotocin-induced diabetic mice. Among the synthesized compounds, compound 19a exerted potency-similarity with dapagliflozin and triggered the hypoglycemic effect in a dose-dependent manner. Besides, compound 19a, even at the high dose of 10 mg/kg, revealed a low risk of hypoglycemia. In further studies, 19a exhibited sustained antihyperglycemic effect without particular side-effects in 30-day chronic diabetic mice studies. Moreover, histological changes in the pancreas of diabetic mice indicated 19a might protect pancreatic β-cell from apoptosis by reducing the damage of glucotoxicity. All of these results demonstrated that compound 19a, with excellent in vivo pharmacological activity and safety profile, was considered to be a promising drug candidate for the treatment of diabetes mellitus.

Key words: blood glucose, *C*-aryl glucosides, diabetes, sodium-dependent glucose cotransporter, urinary glucose

Abbreviations: SGLTs, sodium-dependent glucose cotransporters; EMA, European medicines agency; FDA, food and drug administration; THF, tetrahydrofuran; DMF, N, N-dimethylformamide; STZ, streptozotocin; OGTT, oral glucose tolerance test; AUC, area under the curve; NMR, nuclear magnetic resonance; NMM, N-methylmorpholine; Pyr, pyridine; DMAP, 4-dimethylaminopyridine; SD, standard deviation.

Received 18 December 2014, revised 11 February 2015 and accepted for publication 18 February 2015

The increasing and alarming prevalence of diabetes mellitus along with the undesirable side-effects (such as body weight gain, hypoglycemia, gastric symptoms) associated with many current hypoglycemic agents has motivated a great attempt to evaluate new mechanisms to achieve preferable antidiabetic agents (1,2). Sodium-dependent glucose cotransporters (SGLTs), the prominent ones of novel diabetes targets in the last decade, play a key role in the absorption and reabsorption of glucose from the intestine and kidney (3–5). Among several subtypes identified in the SGLTs, the expression of SGLT2 was found kidney specific, whereas SGLT1 was expressed in the small intestine, heart, brain, and renal tubules (6) and might cause unexpected adverse effects (such as glucose–galactose malabsorption) if inhibited (7). Therefore, selective inhibition of SGLT2 exhibited a safe mechanism to enhance the caloric output associated with weight loss due to the urinary glucose excretion (8), which indicated that selective SGLT2 inhibitor was a highly appreciated approach to the treatment of diabetes mellitus.

A large number of compounds derived from the *C*-aryl glucosides have been reported as SGLT2 inhibitors (Figure 1) (9–17); however, an advisory committee vote against the approval of dapagliflozin in January 2012 for safety concerns (18). It was previously reported that excess quinones and methine-quinones (Figure S1), arose from dapagliflozin *via* oxidative metabolic pathways, might be associated with adverse events such as breast and bladder cancers (19,20). On the other hand, homology modeling and molecular docking demonstrated that the ethoxy oxygen of dapagliflozin was essential to activities or selectivity because a hydrogen bond was formed between the main chain N–H of His80 and the ethoxy oxygen (21). Meanwhile, our previous study also identified the importance of the ethoxy oxygen to activity and selectivity (22,23). Therefore, our chemistry efforts were directed toward decreasing the oxidative metabolism of dapagliflozin and maintaining the hydrogen bond. Many classic strategies have been extensively used to block metabolic hotspots by replacing a hydrogen atom with fluorine or deuterium (19,24,25). Recently, a new strategy, significantly reducing

 doi: 10.1111/cbdd.12547

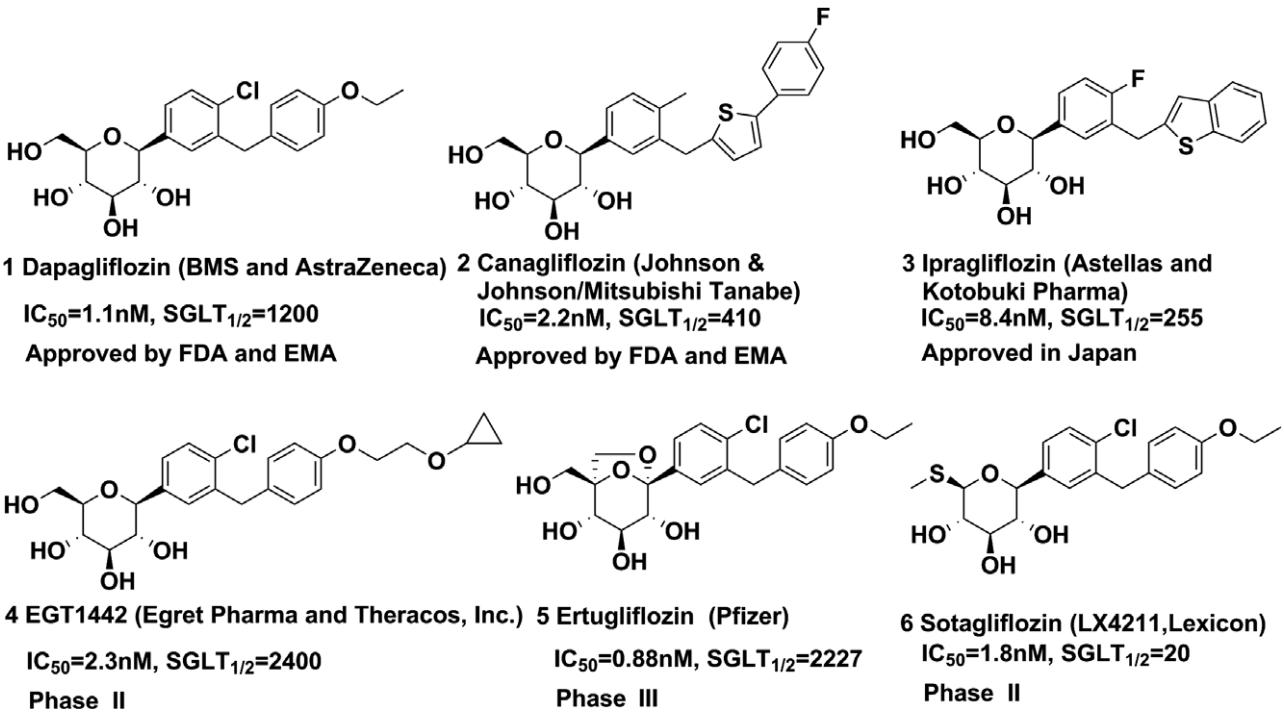

Figure 1: Selected examples of SGLT2 inhibitors.

the oxidative metabolism, was successfully applied to G protein-coupled receptor 40 agonists by introduction of a fluorine, methyl group or cyclization at the ortho position of the phenylpropanoic acid moiety (Figure S2A) (26–28). Herein, with this new perspective, our research was devoted to decrease the oxidative metabolism of dapagliflozin by introducing substituents at the 3′-position or cyclization at 3′, 4′-positions of the distal aryl ring (Figure S2B). In this study, we discovered that the steric, rather than electronic, effect at the 3′-position of the distal aryl ring might influence inhibition activity of SGLTs. Among the synthesized compounds, compound **19a** with good metabolic stability, exhibited excellent *in vivo* pharmacological efficacy and safety profile, was considered to be a promising drug candidate for the treatment of diabetes mellitus.

Methods and Materials

General chemistry

All reagents and solvents were obtained from commercial sources and used without further purification unless otherwise indicated. Purifications by column chromatography were carried out over silica gel (200–300 mesh) and monitored by thin-layer chromatography performed on GF/UV 254 plates and were visualized using UV light at 254 and 365 nm. Melting points were taken on a RY-1 melting-point apparatus and were uncorrected. NMR spectra were recorded on a Bruker ACF-300Q instrument (Bruker BioSpin AG, Fllanden, Switzerland) (300 MHz for ^{1}H NMR and 75 MHz for ^{13}C NMR spectra), chemical shifts are expressed as values relative to tetramethylsilane as internal standard, and coupling constants (*J* values) were given in hertz (Hz). LC/MS spectra were recorded on a Waters liquid chromatography–mass spectrometer system (ESI). Elemental analyses were performed by the Heraeus CHN-O-Rapid analyzer. Dapagliflozin was synthesized as previously reported (9).

General procedure for the synthesis of compounds 16a-h

To a stirred −78 °C solution of **15a-h** (1.0 equiv) in 1: 2 THF/toluene (30 mL) under N_2 was added n-BuLi (2.5 M in hexane, 1.2 equiv) dropwise while keeping the temperature below −70 °C. After 45 min, this solution was transferred by a cannula to a stirred −78 °C solution of 2, 3, 4, 6-tetra-O-trimethylsilyl-β-D-glucolactone **7** (1.5 equiv) in toluene (5 mL) at a rate that maintained the reaction temperature below −70 °C. After 3 h, methanesulfonic acid (0.6 N in MeOH, 3 equiv) was added, whereupon, the reaction was allowed to slowly warm to room temperature overnight. The reaction was then quenched with saturated aqueous $NaHCO_3$ (20 mL) and extracted with EtOAc (3 × 30 mL), the combined organic layers were washed once with saturated brine and dried over anhydrous Na_2SO_4 prior to concentrating using a rotary evaporator, the residue was purified by column chromatography (CH_2Cl_2: MeOH = 30: 1, v/v) to yielded **16a-h** as a glassy off-white amorphous solid.

Synthesis of (3R,4S,5S,6R)-2-(4-chloro-3-(4-ethoxy-3-fluorobenzyl)phenyl)-6-(hydroxymethyl)-2-methoxytetrahydro-2H-pyran-3,4,5-triol (16a)

Yield 60%; mp: 60–62 °C; ^{1}H NMR (300 MHz, DMSO-d_6) δ: 7.52–7.40 (m, 3H, ArH), 7.05–7.01 (m, 1H, ArH), 6.99, 6.97 (dd, J = 1.80 Hz, 8.42 Hz, 1H, ArH), 6.89 (d, J = 8.46 Hz, 1H, ArH), 4.99 (d, J = 5.46 Hz, 2H, 2 × OH), 4.54 (t, J = 5.68 Hz, 1H, -OH), 4.07–3.99 (m, 5H, $ArCH_2Ar$, -OH, -OCH_2), 3.75–3.66 (m, 1H, sugar-OCH_2), 3.47–3.40 (m, 1H, sugar-OCH_2), 3.35–3.05 (m, 4H, 4× OCH), 2.92 (s, 3H, -OCH_3), 1.33 (t, J = 6.96 Hz, 3H, -CH_3).

General procedure for the synthesis of compounds 18a-h

To a stirred −15 °C solution of O-methylglucoside, **16a-h** (1.0 equiv) in 1: 1 CH_2Cl_2/MeCN (20 mL) was added Et_3SiH (1.5 equiv) followed by BF_3·OEt_2(1.2 equiv) at a rate that maintained the reaction temperature below −10 °C; the solution was warm to −10 °C over 10 h prior to quenching with saturated aqueous $NaHCO_3$ (20 mL) and diluted with H_2O (25 mL). The aqueous layer was extracted with EtOAc (3 × 20 mL), and the combined organic layers were washed with H_2O (2 × 10 mL), saturated brine (2 × 15 mL) prior to drying over anhydrous Na_2SO_4, filtration and concentration under reduced pressure yielded a yellow foam. Peracetylation was achieved by addition of Ac_2O (10 equiv) and a catalytic amount of DMAP to a solution of this residue in CH_2Cl_2 (15 mL) and pyridine (10 equiv). After 4 h, the reaction mixture was poured into water (20 mL) and extracted with CH_2Cl_2 (2 × 25 mL). The combined organic layers were washed with 1 N HCl (2 × 15 mL) and saturated brine (2 × 15 mL) prior to drying over anhydrous $MgSO_4$. After filtration and concentration under reduced pressure, the residue was recrystallized from EtOH to yield the desired tetra-acetylated-β-C-glucoside **18a-h** as a white solid.

Synthesis of (2R,3R,4R,5S)-2-(acetoxymethyl)-6-(4-chloro-3-(4-ethoxy-3-fluorobenzyl)phenyl) tetrahydro-2H-pyran-3,4,5-triyl triacetate (18a)

Yield 55%; mp: 132–134 °C; ^{1}H NMR (300 MHz, DMSO-d_6) δ: 7.43 (d, J = 8.49 Hz, 1H, ArH), 7.28 (d, J = 1.89 Hz, 1H, ArH), 7.25 (s, 1H, ArH), 7.05 (t, J = 8.67 Hz, 1H, ArH), 6.99, 6.96 (dd, J = 1.92 Hz, 8.65 Hz, 1H, ArH), 6.90 (d, J = 8.45 Hz, 1H, ArH), 5.35 (t, J = 9.48 Hz, 1H, -OCH), 5.07 (t, J = 9.45 Hz, 1H, -OCH), 4.96 (t, J = 9.64 Hz, 1H, -OCH), 4.66 (d, J = 9.69 Hz, 1H, -OCHAr), 4.10-3.98 (m, 7H, $ArCH_2Ar$, -OCH, 2× OCH_2), 2.01 (s, 3H, CH_3CO), 1.99 (s, 3H, CH_3CO), 1.92 (s, 3H, CH_3CO), 1.70 (s, 3H, CH_3CO), 1.31 (t, J = 6.96 Hz, 3H, -CH_3).

General procedure for the synthesis of compounds 19a-h

To a stirred mixture of tetra-acetylated-β-C-glucoside, **18a-h** (1.0 equiv) in 2:3:1 THF/MeOH/H_2O (18 mL) was added LiOH·H_2O (1.5 equiv). After stirring at room temperature overnight, the volatiles were removed under reduced pressure and the residue, after dissolution in EtOAc (40 mL), was subsequently washed with 5% aqueous $KHSO_4$ (2 × 20 mL) and saturated brine (2 × 15 mL) prior to drying over anhydrous Na_2SO_4. After filtration and concentration using a rotary evaporator, the residue was purified by column chromatography (CH_2Cl_2: MeOH = 30: 1, v/v) to yielded **19a-h** as a glassy off-white amorphous solid.

Synthesis of (2S,3R,4R,5S,6R)-2-(4-chloro-3-(4-ethoxy-3-fluorobenzyl)phenyl)-6-(hydroxymethyl) tetrahydro-2H-pyran-3,4,5-triol (19a)

Yield 91%; mp: 66–68 °C; ^{1}H NMR (300 MHz, DMSO-d_6) δ: 7.38 (d, J = 8.22 Hz, 1H, ArH), 7.35 (d, J = 1.78 Hz, 1H, ArH), 7.26, 7.24 (dd, J = 1.80 Hz, 8.22 Hz, 1H, ArH), 7.07–6.98 (m, 2H, ArH), 6.93 (d, J = 8.40 Hz, 1H, ArH), 4.96 (d, J = 5.53 Hz, 2H, 2× OH), 4.84 (d, J = 9.57 Hz, 1H, -OCHAr), 4.50 (t, J = 5.68 Hz, 1H, -OH), 4.08–3.99 (m, 5H, $ArCH_2Ar$, -OH, -OCH_2), 3.73–3.68 (m, 1H, sugar-OCH_2), 3.49–3.42 (m, 1H, sugar-OCH_2), 3.31–3.08 (m, 4H, 4× OCH), 1.31 (t, J = 6.96 Hz, 3H, -CH_3). ^{13}C NMR (75 MHz, DMSO-d_6) δ: 153.0, 149.8, 139.7, 137.1, 131.8, 130.8, 128.6, 127.5, 124.5, 116.1, 115.8, 114.8, 81.1, 80.6, 78.2, 74.6, 70.2, 64.2, 61.3, 37.4, 14.5. ESI-MS m/z: 449.1 $[M+Na]^+$. Anal. calcd. For $C_{21}H_{24}ClFO_6$: C, 59.09; H, 5.67; Cl, 8.31; F, 4.45; Found: C, 59.01; H, 5.65; Cl, 8.32; F, 4.46.

Biological Studies

Animals

All experiments were performed on male KM mice (18–22 g) that were purchased from Comparative Medicine Centre of Yangzhou University (Jiangsu, China), acclimatized for 1 week before the experiments. The animal room was maintained under a constant 12-h light/dark cycle and rooms were maintained at 23 ± 2 °C and relative humidity 50 ± 10% throughout the experimental period. They were allowed *ad libitum* access to standard pellets and water unless otherwise stated, and the vehicle used for drug administration was 2% ethanol and 2% Tween-80 for all animal studies. All animal procedures were performed in accordance with the applicable institutional and governmental regulations concerning the ethical use of animals.

Statistical analysis of the data

Statistical analyses were performed using specific software (GraphPad InStat version 5.00, GRAPHPAD software, San Diego, CA, USA). Unpaired comparisons were analyzed using the two-tailed Student's t-test, unless otherwise stated.

Hypoglycemic and glucosuria effects of compounds 19a-19h evaluated in normal mice

Normal mice 10 weeks old were fasted overnight (12 h), bled *via* the tail tip, weighted, and randomized into 11 groups (n = 8). Mice were administrated orally with a single doses of vehicle, dapagliflozin (10 mL/kg; 3.68 mol/kg), metformin (10 mL/kg; 200 mg/kg), or compounds **19a**-**19h** (10 mL/kg; 3.68 mol/kg) and subsequently dosed orally with 30% aqueous glucose solution (3 g/kg) after half an hour. Blood samples and urine were collected immediately before drug administration (−30 min), before glucose challenge (0 min), and at 15, 30, 45, 60, and 120 min postdose. The blood glucose was measured by blood glucose test strips (SanNuo ChangSha, ChangSha, China), and the urine glucose was determined by Tes-Tape (Gaoerbao GuangZhou, GuangZhou, China).

Diabetic mice model established by STZ

The mice were made diabetic by a consecutive 5 days intraperitoneal injection of streptozotocin (Sigma, St Louis, MO, USA) at 50 mg/kg, dissolved in fresh cold (4 °C) 0.01 mol/L citrate buffer (pH 4.5). The normal control mice were only injected with the citrate buffer. Five days after STZ injection, development of diabetes was confirmed by measuring blood glucose levels. The mice with overnight fasting blood glucose level 11.1 mmol/L or higher were considered to be diabetic and were used in the experiment.

Oral glucose tolerance test of 19a and 19h explored in STZ-induced diabetic mice

STZ-induced diabetic mice were fasted overnight, bled *via* the tail tip, weighted, and randomized into four groups (n = 6). Mice were dosed orally with single doses of vehicle or dapagliflozin (10 mL/kg; 3.68 mol/kg) or compounds **19a** and **19h** (10 mL/kg; 3.68 mol/kg) and subsequently dosed orally with 30% aqueous glucose solution (3 g/kg) after half an hour. Then, mice were bled at 0, 15, 30, 60, and 120 min postdose to measure blood glucose by blood glucose test strips (SanNuo ChangSha, ChangSha, China).

Hypoglycemic effects of 19a and 19h explored in STZ-induced diabetic mice

Non-fasted STZ-induced diabetic mice were randomized into four groups and placed in cages, and a group of non-fasted normal mice was also taken as a control, then dosed orally with single doses of vehicle, dapagliflozin (10 mL/kg; 3.68 mol/kg), or compounds **19a** and **19h** (10 mL/kg; 3.68 mol/kg). Blood samples were collected from the tail vein immediately before administration (0 h) and at 30 min, 1, 2, 3, 4, 5, and 6 h after administration under fasting conditions to measure blood glucose by blood glucose test strips (SanNuo ChangSha, ChangSha, China).

Dose–response relationship of 19a explored in STZ-induced diabetic mice

To investigate dose–response relationship of **19a**, compound **19a** (0.3, 1, 3, 10 mg/kg) was administered to STZ-induced diabetic mice in the fed condition. Blood glucose levels were then measured for 3 h under fasting conditions, to eliminate the influence of feeding during the experiment.

Effects on normal fasting plasma glucose in normal mice

Ten-week-old male normal mice were fasted overnight and randomized into three groups (n = 6). Compound **19a** (10 mg/kg), glibenclamide (10 mg/kg), or vehicle was orally administered, and blood was collected from tail vein immediately before administration (0 h) and at 30 min, 1, 2, and 3 h after administration to measure blood glucose as described above.

Chronic diabetic mice studies

STZ-induced diabetic mice were dosed daily with the vehicle, dapagliflozin (10 mL/kg; 3.68 mol/kg), or compounds **19a** (10 mL/kg; 3.68 mol/kg) by gavage administration for 30 days, and a group of normal mice was also taken as a control. Animals were dosed at 4:00 PM daily. The body weights were measured every 5 days and the dosage was adjusted according to the most recent body weight. Water and food consumption were measured daily at fixed time intervals. All animals were observed daily and any abnormal state was recorded. Non-fasting blood glucose concentrations were determined on days 0, 5, 10, 15, 20, and 28 at 24 h postdose. Fasting blood glucose concentrations were determined on days 1, 3, 8, 13, 18, and 25 at 12 h postdosing under fasting conditions.

To examine the effects of acute and chronic **19a** treatment on blood glucose levels, the OGTT was performed on days 1, 12, and 29 of treatment. Mice were fasted overnight prior to treatment with a single doses of vehicle, dapagliflozin (10 mL/kg; 3.68 mol/kg), or compounds **19a** (10 mL/kg; 3.68 mol/kg) and subsequently dosed orally with 30% aqueous glucose solution (3 g/kg) after half an hour. Mice were bled *via* tail tip immediately before drug administration, before glucose challenge, and at 15, 30, 60, and 120 min postdose, and the blood glucose was measured by blood glucose test strips (SanNuo ChangSha, ChangSha, China).

At the end of treatment, HbA1c levels in whole blood were determined by automatic biochemical analyzer on day 30, and the pancreases of **19a** (10 mL/kg; 3.68 mol/kg)-treated, dapagliflozin (10 mL/kg; 3.68 mol/kg)-treated, vehicle-treated mice, or normal control mice were isolated immediately after killing and washed with ice-cold saline before fixed in 10% (v/v) formalin. The sections were embedded in paraffin after dehydrate. Four-micron

sections were cut and stained with H&E for histopathological assessment. Islet number was estimated by counting focal islets on five sections for each pancreas, each spaced 245 μm (35 sections) apart. The area of each islet (μm) was determined for each section.

Results and Discussion

Chemistry

The synthesis of the designed compounds **19a-19h** was started from intermediate **15a-15h**. Persilylated gluconolactone **7** was prepared by dropwise trimethylsilyl chloride to commercially available gluconolactone in anhydrous THF and N-methylmorpholine in 99% yield. Compounds **15a-15e** were synthesized starting from **13a to 13e** as shown in Scheme 1. Friedel–Crafts acylation of the starting material **13a-13e** with 5-bromo-2-chlorobenzoyl chloride, formed from commercially available 5-bromo-2-chlorobenzoic acid with oxalyl chloride catalyzed by DMF, generated the desired **14a-14e**, which were isolated in pure from ethanol. Reduction of **14a-14e** by triethylsilane and $BF_3{\cdot}OEt_2$ provided desired intermediate aglycon **15a-15e**.

Compounds **15f-15h** were synthesized starting from phenol **8** as shown in Scheme 2. After stirring at room temperature for 16 h, phenol was alkylated by ethyl chloroacetate in DMF under the action of K_2CO_3. Friedel–Crafts acylation of **9** with 5-bromo-2-chlorobenzoyl chloride, formed from commercially available 5-bromo-2-chlorobenzoic acid with oxalyl chloride catalyzed by DMF, generated the desired **10**, which was isolated in pure from ethanol. Reduction of **10** by triethylsilane and $BF_3{\cdot}OEt_2$ provided **11**. To afford the desired **12,** our initial effort was to try various reaction conditions of Vilsmeier–Haack–Arnold reaction. Unfortunately, there was no reaction detected in compound **11**. We speculated that 5-bromo-2-chlorobenzyl, as a large steric substituent, restrict the reaction. Thus, our ultimate efforts were directed toward stronger reaction condition which obtained by Duff reaction with hexamethylenetetramine and trifluoroacetic acid (29). Then, a mixture of **12**, anhydrous potassium carbonate, and dry DMF was heated at 92–94 °C with stirring for 4 h to generate the desired **13**. Reduction of **13** by $NaBH_4$ and MeOH in reflux anhydrous THF provided desired compound **14**. Alkylation of compound **14** provided desired intermediate aglycon **15f**-**15h**.

The synthesis of the target compounds **19a-19h** is depicted in Scheme 3, and the nascent lithiated aromatic through lithium halogen exchange was added to **7**, yielded a mixture of lactols, which was treated with methanesulfonic acid in methanol to provide the desilylated O-methyl lactols **16a-16h**. Reduction of **16a-16h** by $BF_3{\cdot}OEt_2$ and triethylsilane, followed by peracetylation, obtained tetraacetate **18a-18h** after recrystallization in pure from ethanol. Hydrolysis of **18a-18h** with lithium hydroxide provided target compounds **19a-19h** in high yield.

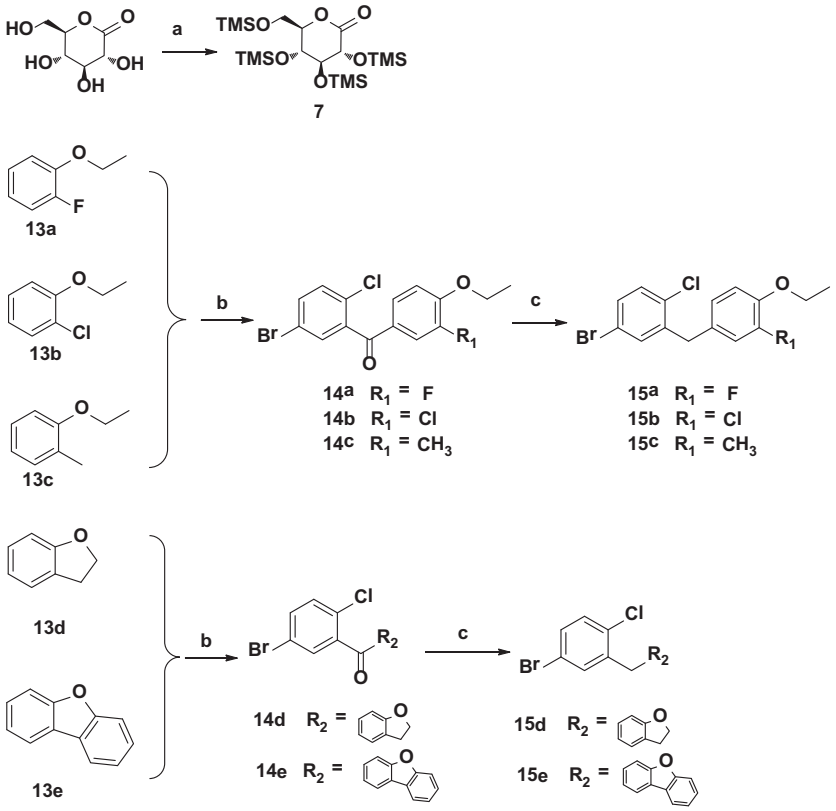

Scheme 1: Synthesis of persilylated gluconolactone **7** and intermediate aglycon **15a-15e**. Reagents and conditions: (a) TMSCl, NMM, THF, 35 °C, 99%; (b) $(COCl)_2$, CH_2Cl_2, DMF, then **13a-13e**, $AlCl_3$, 0 °C, 60–80%; (c) Et_3SiH, $BF_3{\cdot}OEt_2$, CH_2Cl_2, CH_3CN, 25 °C, 90–98%.

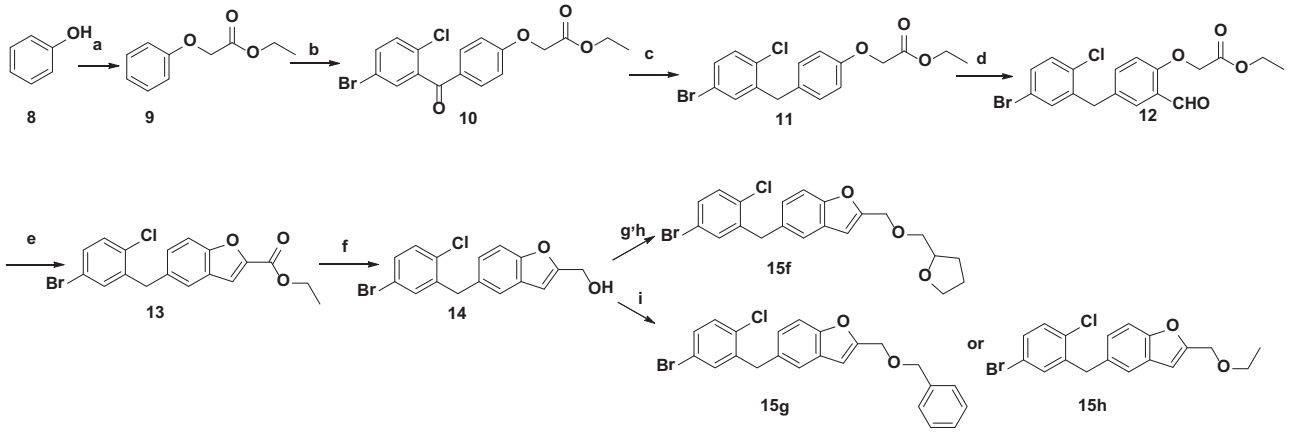

Scheme 2: Synthesis of intermediate aglycon **15f-15h**. Reagents and conditions: (a) K_2CO_3, DMF, rt; (b) $(COCl)_2$, CH_2Cl_2, DMF, then **9**, $AlCl_3$, 0 °C, 55.6%; (c) Et_3SiH, BF_3•OEt_2, CH_2Cl_2, CH_3CN, 25 °C, 72.5%; (d) hexamethylenetetramine, trifluoroacetic acid, reflux; (e) K_2CO_3, DMF, 92–94 °C; (f) $NaBH_4$ and MeOH, THF, reflux; (g) $SOCl_2$, 60 °C; (h) tetrahydrofurfuryl alcohol, KOH, THF; (i) BnBr or bromoethane, KOH, THF.

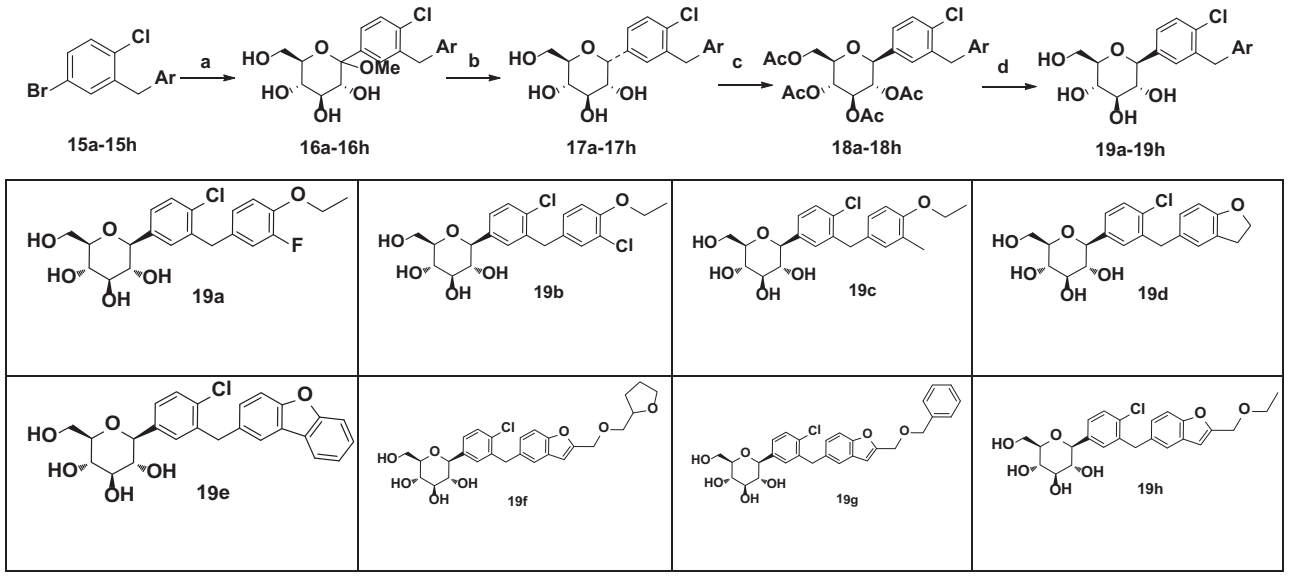

Scheme 3: Synthesis of target compounds **19a-19h**. Reagents and conditions: (a) n-BuLi, THF, toluene, −78 °C, then **7** followed by MeOH, CH_3SO_3H, 20–72%; (b) Et_3SiH, BF_3·OEt_2, CH_2Cl_2, CH_3CN, −10 °C; (c) Ac_2O, pyr, CH_2Cl_2, DMAP, 58–60%, two steps; (d) LiOH·H_2O, THF, H_2O, MeOH, 90–95%.

In vivo *efficacy evaluated in the normal mice*

To estimate the potency of compounds **19a-19h**, the hypoglycemic effects were firstly evaluated in normal mice by oral glucose tolerance test (OGTT). The time-dependent changes of plasma glucose and the area under the curve ($AUC_{0-2\ hr}$) of the blood glucose levels are shown in Figure 2. Compounds with electron-withdrawing fluorine and chlorine and electron-donating methyl group (**19a**, **19b,** and **19c**) were designed to investigate the effects of diverse substitutions in the 3′-position on potency. Meanwhile, the Van der Waals radius of fluorine (**19a**) is close to the size of hydrogen (dapagliflozin), and the size of chlorine (1.75 Å) is close to the size of methyl group (1.80 Å) (30). Therefore, the hypoglycemic effects of dapagliflozin (3′-H) ≈ **19a** (3′-F) > **19b** (3′-Cl) ≈ **19c** (3′-Me) (Figure 2A) suggested that the steric (**19a** vs **19b** and **19c**), rather than electronic (dapagliflozin versus **19a**), effect in the 3′-position might influence inhibition activity of SGLTs. One possible explanation is that incorporation of bulkier substituents such as methyl and chloro changes the favorable conformation of ethoxy group and does great harm to the formation of hydrogen bond between the main chain N–H of His80 and the ethoxy oxygen of the compound.

On the basis of this assumption, our optimized efforts were directed to restrict conformational flexibility of ethoxy

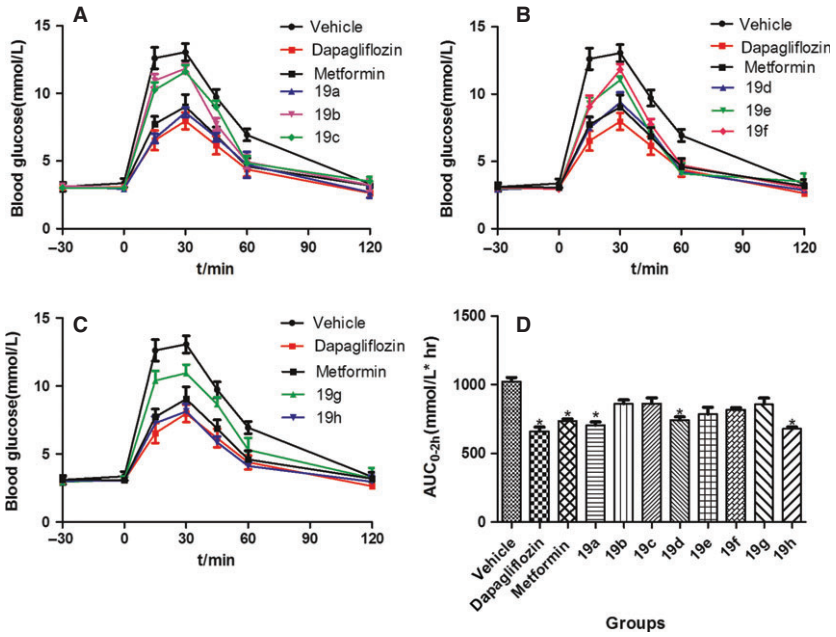

Figure 2: Effects of **19a-19h** on blood glucose levels during an OGTT in normal mice. A, B, and C represent time-dependent changes of plasma glucose. D shows the $AUC_{0-2\ h}$ of blood glucose levels. Values are mean ± SD (n = 8). *p ≤ 0.05 compared to vehicle normal mice by Student's t-test.

group to explore the suitable orientation of oxygen atom, so desired 3′, 4′-cyclization compound **19d** was obtained (Figure 2B). Compared to the **19b** and **19c**, the potency of **19d** was increased obviously but still lower than dapagliflozin; we thought the moderate potency of **19d** could be attributed to deviate from the preferential orientation of oxygen and the lack of hydrophobic effect since in absence of ethyl group. Therefore, we converted dihydrobenzofuran of **19d** into benzofuran to explore the best orientation of oxygen atom. At the same time, three typically hydrophobic groups were selected to further improve the activity: planar aromatic hydrophobic substituent (**19e, 19g**), cycloalkyl hydrophobic group (**19f**), and the small chain alkyl (**19h**). Interestingly, compound **19h** robustly lowered the blood glucose compared with the compound **19d** just as expected. However, tricyclic skeleton such as compound **19e** appeared to diminish the *in vivo* efficacy in mice, likely suggesting that a planar template might be unfavorable. Introduction of a cycloalkyl hydrophobic group (**19f**) or benzyl (**19g**) to the C-2 position of benzofuran demonstrated poor *in vivo* inhibitory activity against SGLTs, suggesting that a simple alkyl chain is more appropriate than bulkier ring structure for this region.

To indirectly elucidate the mechanisms of the novel C-aryl glucosides, the compounds **19a-19h** were selected to investigate the glucosuria in normal mice (Table 1). Dapagliflozin and compounds **19a**, **19d,** and **19h**, which presented good hypoglycemic activities, significantly increased the urinary glucose excretion, while metformin and control group could not. Besides, the urinary glucose of the compounds was consistent with the time-dependent changes of blood glucose. All the result above indicated that these compounds lowered blood glucose by inhibiting SGLTs to reduce the glucose reabsorption in kidney.

Table 1: Urine glucose excretion effects of metformin, dapagliflozin, and **19a-19h** in normal mice

Compound	−30 min	0 min	15 min	30 min	45 min	60 min	120 min
Vehicle	−	−	−	−	−	−	−
Metformin	−	−	−	−	−	−	−
Dapagliflozin	−	++	+++	+++	++++	++++	+++
19a	−	++	+++	+++	++++	++++	+++
19b	−	±	+	+	++	+	+
19c	−	−	±	+	+	−	−
19d	−	+	++	++	+++	++	++
19e	−	−	±	+	+	−	−
19f	−	−	−	+	−	−	−
19g	−	−	±	+	+	+	−
19h	−	++	+++	+++	++++	+++	+++

Symbol represents the mean urine glucose levels of each group (n = 8). −: no glucose; ±: 100 mg/dL; +: 250 mg/dL; ++: 500 mg/dL; +++: 1000 mg/dL; ++++: 2000 mg/dL.

Hypoglycemic effects of 19a and 19h explored in STZ-induced diabetic mice

To further assess antihyperglycemic effects in the diabetic state, STZ-induced diabetic mice were used to evaluate the OGTT of **19a** and **19h**, the most potent inhibitors among our synthetic compounds against SGLTs. As shown in Figure 3A and B, compounds **19a** and **19h** presented potency-similarity with dapagliflozin. Then, long-acting effect was explored in non-fasting STZ-induced diabetic mice (Figure 3C and D). For the first 2 h after dosing, all the two compounds lowered blood glucose almost equivalently, while the hypoglycemic activity of compound **19h** had a significant decrease after 2 h compared to **19a** and dapagliflozin. This result likely suggested that compound **19h** appeared to be susceptible to metabolic inactivation.

Dose–response relationship of 19a explored in STZ-induced diabetic mice

Based on these results above, the most potent compound **19a** was selected to research the dose–response relationship for lowering blood glucose levels. Figure 4A shows that single administration of **19a** (0.3, 1, 3 and 10 mg/kg) dose dependently reduces blood glucose level in STZ-induced diabetic mice. Furthermore, the plasma glucose

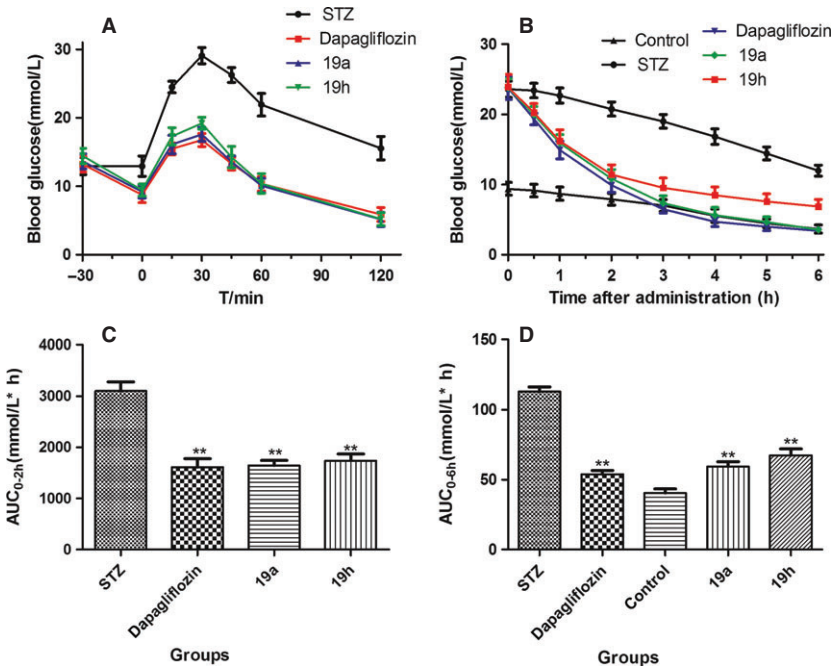

Figure 3: A and B represent time-dependent changes of plasma glucose and $AUC_{0-2\ h}$ of blood glucose levels in OGTT of **19a** and **19h** explored in fasting STZ-induced diabetic mice**,** C and D represent time-dependent changes of plasma glucose and $AUC_{0-6\ h}$ of blood glucose levels in long-acting hypoglycemic effects of compounds **19a** and **19h** explored in non-fasting STZ-induced diabetic mice. Values are mean ± SD (n = 6). **p ≤ 0.01 compared to vehicle STZ mice by Student's t-test.

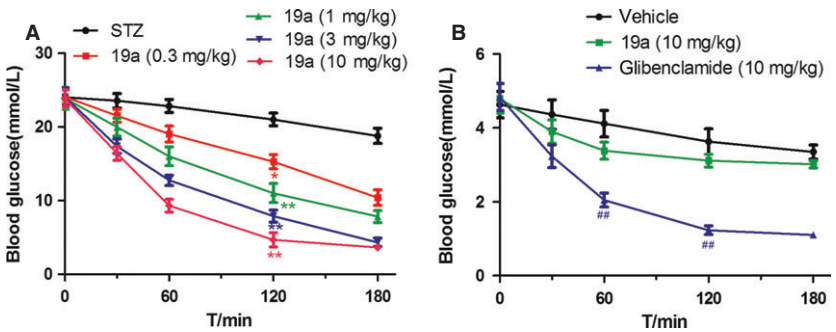

Figure 4: (A) Dose–response relationship of **19a** explored in non-fasting STZ-induced diabetic mice. (B) Effects of **19a** on fasting plasma glucose in normal mice. Values are expressed as mean ± SD for six animals in each group. *p ≤ 0.05, **p ≤ 0.01 compared to vehicle STZ mice by Student's t-test. ##p ≤ 0.01 compared to **19a** by Student's t-test.

curve of **19a** approached to flat after 120 min at the dose of 10 mg/kg. This result might be at least in part rationalized by the low risk of hypoglycemia.

Effects of 19a on fasting plasma glucose in normal mice

Obtaining a positive result in *in vivo* pharmacological study, the risk of hypoglycemia was evaluated in fasting normal KM mice by oral administration of a high dose of **19a** in comparison with glibenclamide to further confirm the above speculation. As shown in Figure 4B, glibenclamide (10 mg/kg) lowered plasma sugar levels far below normal fasting levels in KM mice. In contrast, compound **19a**, even at the high dose of 10 mg/kg, only slightly reduced fasting glucose levels in KM mice, and the change of blood glucose levels was much smaller compared to that caused by administration of glibenclamide. Thus, our results indicated that compound **19a** not only effectively improved hyperglycemia in the diabetic state, but also

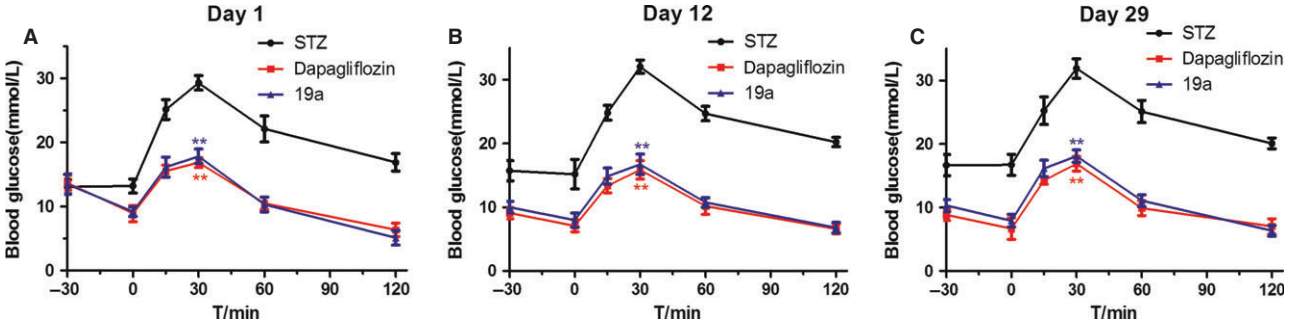

Figure 5: The OGTT of compound **19a** in fasting STZ-induced diabetic mice after long-term treatment. Dapagliflozin, **19a**, or vehicle was orally administered to STZ-induced diabetic mice once daily for 30 days. The blood glucose levels were determined on treatment day 1, 12, and 29. Values are expressed as mean ± SD for six animals in each group. **p ≤ 0.01 compared to vehicle STZ mice by Student's *t*-test.

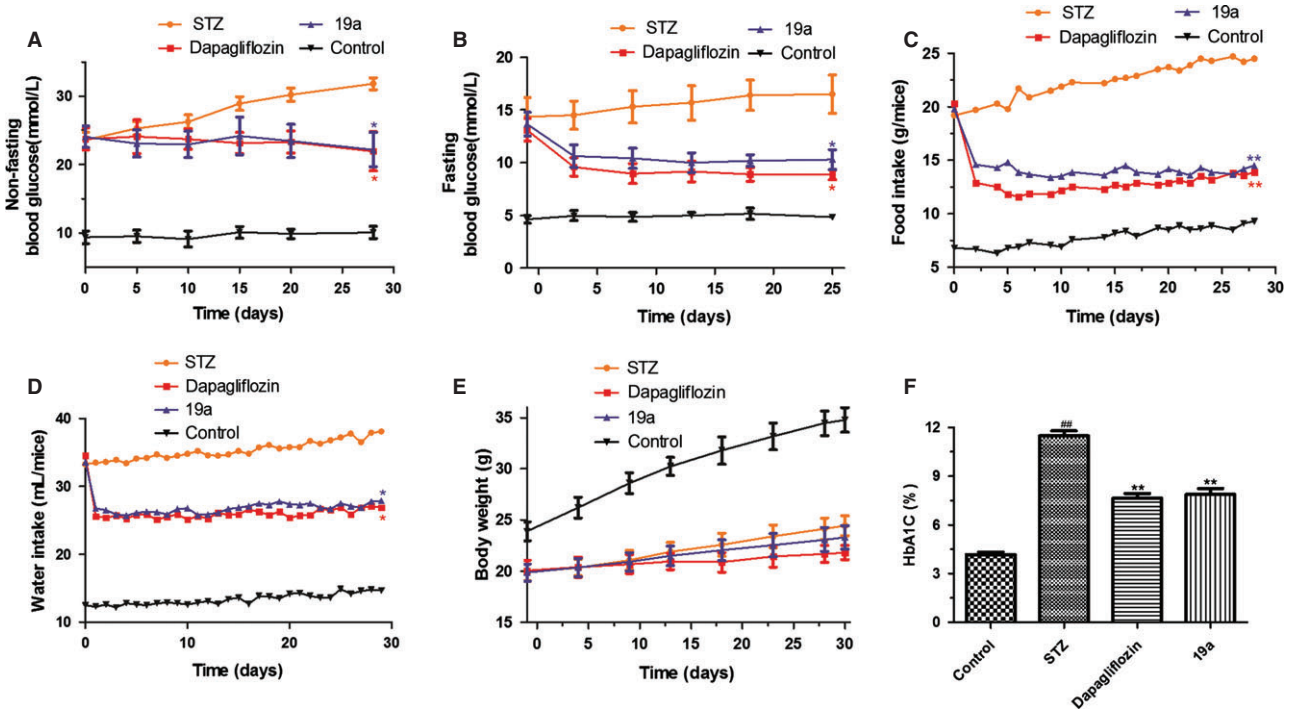

Figure 6: The antihyperglycemic effects of chronic **19a** treatment on non-fasting blood glucose levels at 24 h postdose (A), fasting blood glucose levels at 12 h postdosing under fasting conditions (B), food intake (C), water intake (D), body weight (E), and the levels of HbA1c (F) in STZ-induced diabetic mice. Dapagliflozin, **19a**, or vehicle was orally administered to STZ-induced diabetic mice once daily for 30 days. Food consumption, water intake, and body weight were measured at fixed time intervals. Values are expressed as mean ± SD for six animals in each group. ##p ≤ 0.01 compared to control by Student's *t*-test. *p ≤ 0.05, **p ≤ 0.01 compared to vehicle STZ mice by Student's *t*-test.

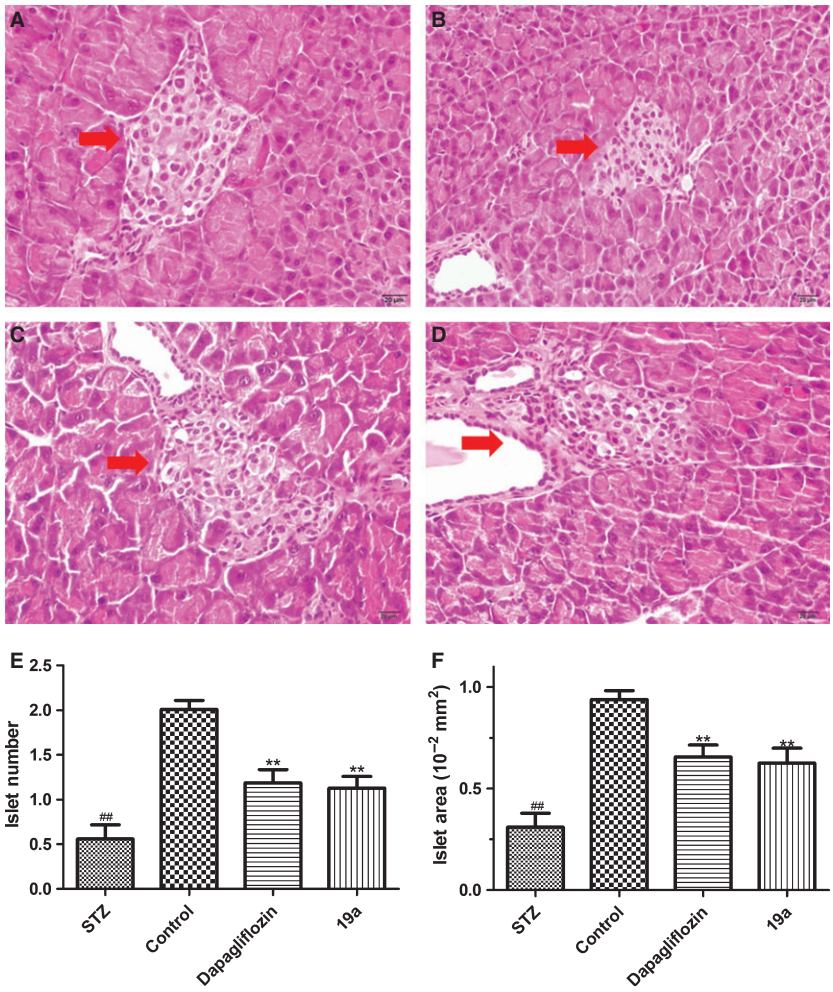

Figure 7: Representative pancreatic islet of mice of each group, red arrow shows pancreatic β-cell. (A). Representative pancreatic islet of normal control mice. (B). Representative pancreatic islet of diabetic control mice showed depletion of islets and uneven distribution of cell nuclei. (C). Representative pancreatic islet of dapagliflozin-treated mice showed improved islets. (D). Representative pancreatic islet of **19a-**treated mice showed improved islets. (E). Representative the number of islet per mouse for islet observed with the 100 times magnifying glass. (F). Representative islet area observed with the 200 times magnifying glass. Values are mean ± SD (n = 6), $^{\#\#}p \leq 0.01$ compared to control by Student's t-test. $^{**}p \leq 0.01$ compared to vehicle STZ-induced diabetic mice by Student's t-test.

revealed a low risk of hypoglycemia, a serious side-effect to sulfonylureas such as glibenclamide.

Chronic diabetic mice studies

On the basis of the promising *in vivo* pharmacological and excellent safety profile of compound **19a**, a 30-day chronic **19a** treatment study was subsequently carried out in STZ-induced diabetic mice to assess whether the compound could maintain long-term effects. In this study, dapagliflozin, **19a**, and vehicle were orally administered to STZ-induced diabetic mice once daily for 30 days, the OGTT was performed on days 1, 12, and 29 of treatment. As shown in Figure 5, on the first day of treatment, the acute administration of dapagliflozin and **19a** caused a 44.6% and 44.9% decrease in the glucose $AUC_{0-2\ h}$ values. On day 12 and 29 of treatment, dapagliflozin or **19a** showed similar effects, with a decrease in the glucose $AUC_{0-2\ h}$ values of 55.4% and 52.3% (day 12), and 55.5% and 51.6% (day 29), respectively. This demonstrated that the antihyperglycemic effect of compound **19a** was sustained throughout the treatment.

Furthermore, the non-fasting and fasting blood glucose levels were determined throughout the research. As shown in Figure 6A and B, the non-fasting and fasting glucose levels of STZ-induced diabetic mice were significantly higher than those of the normal control group. The non-fasting and fasting blood glucose levels were reduced significantly in the oral administration of compound **19a** and dapagliflozin compared with the vehicle-treated controls after 5 days of treatment. Thereafter, the blood glucose levels remained steady throughout the treatment. The food consumption and water intake, which shared a similar change as fasting blood glucose levels, were improved in the treated group of compound **19a** and dapagliflozin

(Figure 6C and D). The treated groups caused slightly reductions in the body weight after 30 days of treatment compared with vehicle-treated controls (Figure 6E). After a 30-day chronic treatment, STZ-induced diabetic mice treated with compound **19a** and dapagliflozin had HbA1c values of 7.88% ± 0.32% and 7.64% ± 0.25%, respectively, demonstrating a significant improvement compared with vehicle-treated group (11.47% ± 0.29%) (Figure 6F).

In this chronic **19a** treatment study, no particular side-effects were observed at compound **19a**-treated group, indicating the possibility that minimized off-target pharmacology and metabolic toxicity.

Histological changes in the pancreas of diabetic mice

Freshly isolated islets from normal control, vehicle-, dapagliflozin-, and compound **19a-**treated STZ-induced diabetic mice (30-day treatment) were counted and histologically assessed. As shown in Figure 7, the cytoplasm and nuclear in the islet of the STZ-induced diabetic mice appeared to be lytic and shrunken compared with normal mice. Dapagliflozin- and compound **19a**-treated groups exhibited a significant improvement in islet number and area compared with vehicle-treated STZ-induced diabetic mice. These results indicated that compound **19a** might protect pancreatic β-cell from apoptosis by reducing the damage of glucotoxicity.

Conclusions and Future Directions

We have designed and synthesized a series of novel *C*-aryl glucosides with various substituents at the 3′-position and cyclization at 3′, 4′-positions of the distal aryl ring, and the most potent inhibitors **19a** and **19h** among our synthetic compounds were selected to evaluate in the normal and STZ-induced diabetic mice. Although the hypoglycemic activity of **19h** had a significant decrease after 120 min owing to be susceptible to metabolic inactivation, the current chemistry shown in here allowed us to further modify the structure of **19h** to enhance the metabolic stability. In further studies, the selected compound **19a** exhibited sustained antihyperglycemic effect without particular side-effects in 30-day chronic diabetic mice studies. Moreover, histological changes in the pancreas of diabetic mice indicated **19a** might protect pancreatic β-cell from apoptosis by reducing the damage of glucotoxicity. All of these results demonstrated that compound **19a** was meaningful for further investigation as a drug candidate for the treatment of diabetes mellitus.

Acknowledgments

This work was supported by grants from the National Natural Science Foundation of China (No. 81172932 and No. 81273376) and the Natural Science Foundation of Jiangsu Province (No. BK2012356).

References

1. Levetan C. (2007) Oral antidiabetic agents in type 2 diabetes. Curr Med Res Opin;23:945–952.
2. Phung O.J., Scholle J.M., Talwar M., Coleman C.I. (2010) Effect of noninsulin antidiabetic drugs added to metformin therapy on glycemic control, weight gain, and hypoglycemia in type 2 diabetes. JAMA;303:1410–1418.
3. Wright E.M. (2001) Renal Na+-glucose cotransporters. Am J Physiol-Renal;280:10–18.
4. Jurczak M.J., Lee H.Y., Birkenfeld A.L., Jornayvaz F.R., Frederick D.W., Pongratz R.L., Zhao X., Moeckel G.W., Samuel V.T., Whaley J.M., Shulman G.I., Kibbey R.G. (2011) SGLT2 deletion improves glucose homeostasis and preserves pancreatic β-cell function. Diabetes;60:890–898.
5. Chao E.C., Henry R.R. (2010) SGLT2 inhibition-a novel strategy for diabetes treatment. Nat Rev Drug Discov;9:551–559.
6. Wright E.M., Loo D.D., Hirayama B.A. (2011) Biology of human sodium glucose transporters. Physiol Rev;91:733–794.
7. Martín M.G., Turk E., Lostao M.P., Kerner C., Wright E.M. (1996) Defects in Na+/glucose cotransporter (SGLT1) trafficking and function cause glucose-galactose malabsorption. Nat Genet;12:216–220.
8. List J.F., Whaley J.M. (2011) Glucose dynamics and mechanistic implications of SGLT2 inhibitors in animals and humans. Kidney Int;79:20–27.
9. Meng W., Ellsworth B.A., Nirschl A.A., McCann P.J., Patel M., Girotra R.N., Wu G. *et al.* (2008) Discovery of dapagliflozin: a potent, selective renal sodium-dependent glucose cotransporter 2 (SGLT2) inhibitor for the treatment of type 2 diabetes. J Med Chem;51:1145–1149.
10. Nomura S., Sakamaki S., Hongu M., Kawanishi E., Koga Y., Sakamoto T., Yamamoto Y., Ueta K., Kimata H., Nakayama K., Tsuda-Tsukimoto M. (2010) Discovery of canagliflozin, a novel C-glucoside with thiophene ring, as sodium-dependent glucose cotransporter 2 inhibitor for the treatment of type 2 diabetes mellitus. J Med Chem;53:6355–6360.
11. Imamura M., Nakanishi K., Suzuki T., Ikegai K., Shiraki R., Ogiyama T., Murakami T. *et al.* (2012) Discovery of Ipragliflozin (ASP1941): a novel C-glucoside with benzothiophene structure as a potent and selective sodium glucose co-transporter 2 (SGLT2) inhibitor for the treatment of type 2 diabetes mellitus. Bioorg Med Chem;20:3263–3279.
12. Zhang W., Welihinda A., Mechanic J., Ding H., Zhu L., Lu Y., Deng Z., Sheng Z., Lv B., Chen Y., Roberge J.Y., Seed B., Wang Y.X. (2011) EGT1442, a potent and selective SGLT2 inhibitor, attenuates blood glu-

cose and HbA(1c) levels in db/db mice and prolongs the survival of stroke-prone rats. Pharmacol Res;63:284–293.
13. Mascitti V., Maurer T.S., Robinson R.P., Bian J., Boustany-Kari C.M., Brandt T., Collman B.M. *et al.* (2011) Discovery of a clinical candidate from the structurally unique dioxa-bicyclo[3.2.1]octane class of sodium-dependent glucose cotransporter 2 inhibitors. J Med Chem;54:2952–2960.
14. Goodwin N.C., Mabon R., Harrison B.A., Shadoan M.K., Almstead Z.Y., Xie Y., Healy J. *et al.* (2009) Novel L-xylose derivatives as selective sodium-dependent glucose cotransporter 2 (SGLT2) inhibitors for the treatment of type 2 diabetes. J Med Chem;52:6201–6204.
15. Kasichayanula S., Liu X., LaCreta F., Griffen S.C., Boulton D.W. (2014) Clinical pharmacokinetics and pharmacodynamics of dapagliflozin, a selective inhibitor of sodium-glucose co-transporter type 2. Clin Pharmacokinet;53:17–27.
16. Freiman J., Ruff D., Frazier K., Combs K., Turnage A., Shadoan M., Powell D., Zambrowicz B., Brown P. (2010) LX4211, a dual SGLT2/SGLT1 inhibitor, shows rapid and significant improvements in glycemic control over 28 days in patients with type 2 diabetes (T2DM). Diabetes;59:511.
17. Zambrowicz B., Freiman J., Brown P., Frazier K., Turnage A., Bronner J., Ruff D. *et al.* (2012) LX4211, a dual SGLT1/SGLT2 inhibitor, improved glycemic control in patients with type 2 diabetes in a randomized, placebo-controlled trial. Clin Pharmacol Ther;92:158–169.
18. Mayer P. (2012) Chances and risks of SGLT2 inhibitors. N-S Arch Pharmacol;385:551–554.
19. Xu G., Lv B., Roberge J.Y., Xu B., Du J., Dong J., Chen Y. (2014) Design, synthesis, and biological evaluation of deuterated C-aryl glycoside as a potent and long-acting renal sodium-dependent glucose cotransporter 2 inhibitor for the treatment of type 2 diabetes. J Med Chem;57:1236–1251.
20. Obermeier M., Yao M., Khanna A., Koplowitz B., Zhu M., Li W., Komoroski B., Kasichayanula S., Discenza L., Washburn W., Meng W., Ellsworth B.A., Whaley J.M., Humphreys W.G. (2010) In vitro characterization and pharmacokinetics of dapagliflozin (BMS-512148), a potent sodium-glucose cotransporter type II inhibitor, in animals and humans. Drug Metab Dispos;38:405–414.
21. Nakka S., Guruprasad L. (2012) Structural insights into the active site of human sodium dependent glucose co-transporter 2: homology modelling, molecular docking, and 3D - QSAR studies. Aust J Chem;65:1314–1324.
22. Tang C., Zhu X., Huang D., Zan X., Yang B., Li Y., Du X., Qian H., Huang W. (2012) A specific pharmacophore model of sodium-dependent glucose co-transporter 2 (SGLT2) inhibitors. J Mol Model;18:2795–2804.
23. Wang X., Li Y., Yang B., Li Z., Huang W., Qian H. (2014) *C*-Aryl glucosides with substituents at the distal aryl ring as sodium-dependent glucose co-transporters inhibitors for the treatment of diabetes mellitus. Chem Biol Drug Des;86:246–253.
24. Meanwell N.A. (2011) Synopsis of some recent tactical application of bioisosteres in drug design. J Med Chem;54:2529–2591.
25. Chauret N., Guay D., Li C., Day S., Silva J., Blouin M., Ducharme Y., Yergey J.A., Nicoll-Griffith D.A. (2002) Improving metabolic stability of phosphodiesterase-4 inhibitors containing a substituted catechol: prevention of reactive intermediate formation and covalent binding. Bioorg Med Chem Lett;12:2149–2152.
26. Negoro N., Sasaki S., Mikami S., Ito M., Suzuki M., Tsujihata Y., Ito R. *et al.* (2010) Discovery of TAK-875: a potent, selective, and orally bioavailable GPR40 agonist. ACS Med Chem Lett;1:290–294.
27. Negoro N., Sasaki S., Ito M., Kitamura S., Tsujihata Y., Ito R., Suzuki M. *et al.* (2012) Identification of fused-ring alkanoic acids with improved pharmacokinetic profiles that act as G protein-coupled receptor 40/free fatty acid receptor 1 agonists. J Med Chem;55:1538–1552.
28. Negoro N., Sasaki S., Mikami S., Ito M., Tsujihata Y., Ito R., Suzuki M. *et al.* (2012) Optimization of (2,3-dihydro-1-benzofuran-3-yl)acetic acids: discovery of a non-free fatty acid-like, highly bioavailable G protein-coupled receptor 40/free fatty acid receptor 1 agonist as a glucose-dependent insulinotropic agent. J Med Chem;55:3960–3974.
29. Smit W.E. (1972) Formylation of aromatic compounds with hexamethylenetetramine and trifluoroacetic acid. J Org Chem;37:3972–3973.
30. Bondi A. (1964) van der Waals volumes and radii. J Phys Chem;68:441–451.

Supporting Information

Additional Supporting Information may be found in the online version of this article:

Appendix S1. Experimental details and characterization for the synthesized compounds **19a-19h**.
Appendix S2. **Figure S1.** Possible oxidative metabolic route of dapagliflozin. Solid lines express determined metabolites, the dotted line express predicted metabolites. **Figure S2.** (A) Takeda's strategy to resistant to β-oxidation and improve PK profiles by introduction of substituents or cyclization at the ortho position of the phenylpropanoic acid moiety. (B) Our strategy might to decrease the oxidative metabolism of dapagliflozin.